BioCore
Exploring Scientific Community

International Journal of Nanotechnology in Medicine & Engineering

Research Article
ISSN 2474-8811

Uptake Of Diamond Nanoparticles Blocks Inflammatory Responses in Macrophages

Deepika Bhardwaj[1],Rajiv K. Saxena[1]*

[1]Faculty of Life Sciences and Biotechnology South Asian University, New Delhi, India

Abstract

Current study focuses on the interactions between nanodiamonds and macrophages.Confocal microscopy studies indicated that carboxylated fluorescent nanodiamonds (cFNDs) were efficiently internalized by RAW 264.7 and MH-S macrophage cell lines and were essentially localized in the cytoplasmic area. BCG induced potent inflammatory response in the two macrophage cell lines and carboxylated nanodiamonds (cNDs) significantly inhibited this inflammatory response. Potent inhibitory effect of cNDs was found on the BCG induced production of reactive oxygen species (ROS) and nitric oxide (NO) by both macrophage cell lines. Using quantitative Real time PCR, we found that the treatment with cNDs led to considerable downregulation in expression of BCG induced pro-inflammatory genes- COX-2, iNOS, TNF-α, IL-6 and IL-1β at transcriptional level. Downregulation in expression of BCG induced COX-2 by cNDs was further confirmed at translational level using Western blotting. Using Gelatin zymography we further demonstrated marked reduction in BCG induced release of Matrix Metalloproteinases MMP-2 and MMP-9 by cNDs. Collectively, our results indicate a potent anti-inflammatory effect of cNDs in alleviating BCG induced inflammatory responses in macrophage cell lines. These results suggest that use of nanodiamonds may be explored for suppressing inflammatory responses at the level of macrophages.

Keywords: Nanodiamonds, BCG, inflammation, Macrophages, Flow Cytometry,Confocal microscopy, ROS, NO, COX-2, MMPs.

Corresponding author: Rajiv K. Saxena

Faculty of Life Sciences and Biotechnology,South Asian University, Akbar Bhawan, Chanakyapuri,New Delhi, India

E-mail: rajivksaxena@hotmail.com

Citation: Deepika Bhardwaj and Rajiv K. Saxena (2020), Uptake of diamond nanoparticles blocks inflammatory responses in macrophages. Int J Nano Med & Eng. 5:4

Received: August 19,2020
Accepted: August 24, 2020
Published: October 20, 2020

Introduction

Nanodiamonds represent a novel category of carbon nanoparticles that are approximately 2-8 nm in diameter (1, 2). The core of nanodiamonds comprises of sp3 hybridized carbon atoms while the surface is characterised by presence of sp2 hybridized graphitic carbon atoms that allows easy functionalization with oxygenic functional groups like carboxyl, hydroxyl and keto groups (3). Due to their unique physio-chemical properties, and possibility of easy surface tagging with various chemical groups and drugs, nanodiamonds have become an attractive candidate in diagnostics, imaging, and as therapeutic agents in biomedicine (4-8). Nanodiamonds can be made fluorescent resistant to photo-bleaching by creating nitrogen-vacancy centres in the diamond lattice (9). The resulting fluorescent nanodiamonds (FNDs) are being used as efficient fluorescent probes for in vitro and in vivo imaging (10-14). As such, nanodiamonds do not have many surface groups like -COOH, -NH2 etc, that would render them charged, but the sp2 carbon surface of nanodiamonds may absorb oxonium ions (H30+) from aqueous medium and this protonation results in a net positive zeta potential on pristine nanodiamonds (15). Functionalization of surface sp2 carbon atoms with negatively charged carboxyl group imparts a negative charge to nanodiamonds and the carboxyl group may be exploited to couple a variety of drugs and molecules to nanodiamond cell surface. What further adds to the attractiveness of nanodiamonds in biomedical application is the fact that they are rather inert biologically and do not show significant toxicity in human and animal systems (16, 12, 17, 18). A number of studies have demonstrated the interaction of nanodiamonds with different types of cells (16, 19-23). Non-toxicity and bio-compatibility of nanodiamonds has been demonstrated for 293-T human kidney cells (19), Neuroblastoma, alveolar macrophages and keratinocytes (20), HepG2, HeLa cells (21), Mouse and human

pluripotent embryonal carcinoma (22), A549 human lung epithelial cells (23) and Human/rat red blood cells (16). Nanodiamonds also do not cause significant toxic response when administered in vivo (12, 17, 18). Inflammation is a defensive response of the host against infections and tissue damage and is characterized by a cascade of events including vasodilation and recruitment of immune cells and plasma proteins to the site of infection (24). Since many toxic mediators released during inflammation to eliminate pathogens can also damage the bystander host cells, unconstrained inflammatory response can cause serious cell and tissue damage. Macrophages have a key role in initiating the inflammatory response (25) and drugs and agents that downregulate the inflammatory response in macrophages may prove to be beneficial in containing tissue damage that may occur in chronic inflammation. In this study, we demonstrate that nanodiamonds are internalized by macrophages and significantly block the induction of an inflammatory response to BCG. Two murine macrophage cell lines RAW 264.7 and MH-S were used in this study and all eight parameters of inflammation that we studied (ROS and nitric oxide production, upregulation of COX-2, iNOS, TNF-α, IL-6, IL-1β genes and release of matrix metalloproteinases MMP-2 and MMP-9), were markedly inhibited by carboxylated nanodiamonds (cNDs). These results suggest that use of cNDs may be further explored as an agent that suppresses inflammatory responses initiated at the level of macrophages.

Materials and Methods

Cells

RAW 264.7 (a murine peritoneal macrophage cell line) and MH-S (a murine lung alveolar macrophage cell line) cells obtained from American Type Cell Culture, were cultured in DMEM and RPMI 1640 culture medium respectively supplemented with 2 mM glutamine, 4.5 g glucose per litre, 10 mM HEPES buffer pH 7.2, gentamycin (0.5 mg/ml) and fetal bovine serum (10% V/V).

Nanodiamonds and their characterization

Carboxylated fluorescent nanodiamonds (cFNDs) (catalog no. NDNV100nmHiCOOH10ml) and carboxylated nanodiamonds (cNDs) (catalog no. ND-H20-15nm-II-100ml) were obtained from Adamas Nanotechnologies, USA. Using Zetasizer equipment, (Nano ZS90, Malvern instruments, Malvern, UK) cFNDs suspended in water were found to have an average size of 77.4 rnm and average zeta potential of -32.8 mV while the corresponding values for cNDs were 24.9 rnm and -42mV respectively (Supplementary Fig. 1). Fluorescent nanodiamonds cFNDs containing nitrogen vacancies (NV centres) were used for uptake studies using Confocal microscopy. To study the effects of NDs on different parameters of inflammation in macrophage cell lines, cNDs were used.

Reagents and other supplies

Bio-Rad Clarity Western ECL substrate and 2',7'-Dichlorofluorescin diacetate (DCFDA) were procured from Sigma Aldrich, USA. N-1-napthylethylenediamine dihydrochloride (NED), sulfanilamide, sodium nitrite and polyclonal antibody against mouse COX-2 (Item no. 160126) were obtained from Cayman Chemicals, USA. SYBR-iTAQ Universal SYBR Green super mix was purchased from Bio-Rad Laboratories (California, USA). cDNA Synthesis kit and RNA Iso Plus Trizol were purchased from DSS TaKara, India. DMEM and RPMI 1640 culture medium supplemented with glutamine (2 mM), HEPES buffer pH 7.2 (10 mM), gentamycin (10 µg/ml), fetal bovine serum (FBS) (10% V/V), Middlebrook 7H9 media and OADC supplements were purchased from Himedia, India.

Culture of BCG

BCG was cultured in Middlebrook 7H9 liquid media supplemented with 10% OADC supplements. Growth was monitored by measuring absorbance of the bacterial suspension at 600 nm. Viability and colony forming units (CFU) count was determined by plating on 7H11 agar OADC plates. Autoclaved BCG preparations were obtained by autoclaving the BCG suspensions at 121°C and 15 psi for 60 minutes. Before use, the autoclaved BCG suspensions were passed through a syringe fitted with 26-gauge needle to break clumps.

Confocal Microscopy

To study the uptake and intercellular localization of the cFNDs,RAW 264.7 and MH-S cells were cultured [0.1×106/ml/well] on a coverslip in a 12 well culture plate, incubated with 10 µg/ml of cFNDs for 12 hours, washed twice with PBS and fixed using 4% paraformaldehyde on ice for 10 minutes. The fixed cells were washed thoroughly to get rid of any residual paraformaldehyde and nuclei were counterstained with Hoechst 33342 dye as described before (26). Coverslips were mounted onto the glass slide with 50% glycerol and examined on a Nikon A1R Confocal Laser Scanning Microscope.

Estimation of reactive oxygen species (ROS) and nitric oxide (NO)

ROS generation in the two cell lines was assessed by using fluorogenic dye, 2',7'-Dichlorofluorescin diacetate (DCFDA). For flow cytometry studies to detect the production of ROS, RAW 264.7 and MH-S cells were cultured [0.1×106/ml/well] in 12 well plate with and without various treatments for 12 hours. The cells were trypsinized, washed twice with PBS, and pelleted cells were incubated in fresh media containing 5 µM DCFDA for 30 minutes in the dark at 37°C. ROS produced by the cells brings about oxidation of DCFDA to form fluorescent product DCF (2', 7' dichlorofluorescein), which was estimated by flow cytometry. Nitric oxide (NO) released into culture supernatants was measured by using Griess reagent as described elsewhere (27). Culture supernatants were mixed 1:1 (v/v) with Griess reagent and the color generated after 15-minute incubation at room temperature was read in an ELISA reader at 540 nm.

Real time PCR (RT-PCR):

RT-PCR was carried out as described before (28). Briefly, cells to be tested were washed with cold PBS and incubated with the TRIzol reagent to extract total RNA. cDNA was synthesized using 2 µg total RNA with a cDNA synthesis kit. Forward and reverse sequences of primers were:

β-actin[GGAGGGGGTTGAGGTGTT, GTGTGCACTTTTATTGGTCTCAA];
COX-2 [TGAGTGGGGTGATGAGCAAC, TTCAGAGGCAATGCGGTTCT]
iNOS [GGCAGCCTGTGAGACCTTTG, GCATTGGAAGTGAAGCGTTTC]
TNF-α [GACAAGCCTGTAGCCCACG, TGTCTTTGAGATCCATGCCGT]
IL-6 [ACAAAGCCAGAGTCCTTCAGAG, GAGCATTGGAAATTGGGGTAGG]
IL-1β [ATGCCACCTTTTGACAGTGATG, TGTGCTGCTGCGAGATTTGA]

Reaction volume of 10 µl was used for the amplification consisting of 2.5 µl of ten-fold diluted cDNA, 5 µl SYBR green, 0.2 µl (10 mM) of each primer and sterile distilled water. Cycling condition was as follows: 10 min at 95°C and 40 cycles of 15 sec at 95°C, 30 sec at 60°C and the melt curve with single reaction cycle with the following conditions: 95°C for 15 sec, 60°C for 1 min and dissociation at 95°C for 15 sec. After the amplification, the cycle threshold (Ct) values were obtained and normalized to the value of housekeeping gene β-actin. The relative expressions of the target genes were calculated using the 2-ΔΔCt method.

Western Blotting

Western blot analysis was carried out as described before (29). Briefly, RAW 264.7 and MH-S cells were cultured with or without 100 µg/ml of cNDs and/or Autoclaved BCG MOI 100:1 for 24 hours. Cells were washed twice with ice-cold PBS and incubated in RIPA lysis buffer containing

a cocktail protease inhibitor mixture at 4°C for 20 minutes and then stored at -80 degrees overnight. Next day, cell lysates were sonicated 3 three times for 10 sec each and analysed for protein content using the BCA protein assay kit (Thermo Fisher scientific). Samples containing 30 µg/µl of cell lysate proteins per lane were resolved on SDS-PAGE (10% sodium dodecyl sulfatepolyacrylamide gel electrophoresis) along with pre-stained protein ladder and transferred onto PVDF membranes (Invitrogen). The transferred membranes were blocked for 2 hours using 5% BSA in TBST (25 mm Tris-HCl, pH 7.4, 125 mm NaCl, 0.05% Tween 20) and incubated with COX-2 primary antibody at 4°C overnight. Membranes were washed thrice with TBST for 5 minutes and incubated with horseradish peroxidase coupled isotype-specific secondary antibody for 1 hour at room temperature. The immune complexes were detected by enhanced chemi-luminescence detection system (Bio-Rad) and quantified using NIH Image J software.

Gelatin Zymography for MMP-2 and MMP-9

Protocol used for zymography has been described elsewhere (30). Briefly, 0.1x106 RAW 264.7 and MH-S cells were cultured in a 12 well cell culture plate with or without 100 µg/ml cNDs and/or Autoclaved BCG MOI 100:1 for 12 hours in serum-free media. Supernatants were mixed with 5X nonreducing sample buffer and subjected to electrophoresis on 7.5% SDS-PAGE containing 4 mg/ml gelatin. After washing with the washing buffer for 30 minutes, the gel was incubated in the incubation buffer at 37 °C for 24 hours. Gels were stained with staining solution and were de-stained. The gelatinolytic activity of samples was detected as clear band against blue background. The bands were visualized using a Bio-Rad gel scanner and quantified using NIH Image J software.

Statistical Analysis

All experiments were repeated at least three times. Results are expressed as Mean ±SEM. The paired t-test was performed to define the significance of all the experiments. Statistical analyses were performed using Sigma Plot software (Systat software, San Jose, CA).

Results

Uptake of cFNDs by RAW 264.7 and MH-S cells

We have previously shown that BCG is efficiently taken up by macrophages (31, 32). To study the uptake of cFNDs, RAW 264.7 and MH-S cells were incubated with cFNDs for 12h. Confocal microscopy results in Figure 1 clearly show that almost all cells had taken up cFNDs that appear to be localized essentially in the cytoplasmic area. Z-sectioning data at different depths (2 µm, 2.5 µm and 3 µm) further confirmed that cFNDs were present inside the macrophage cells (Figure 1).

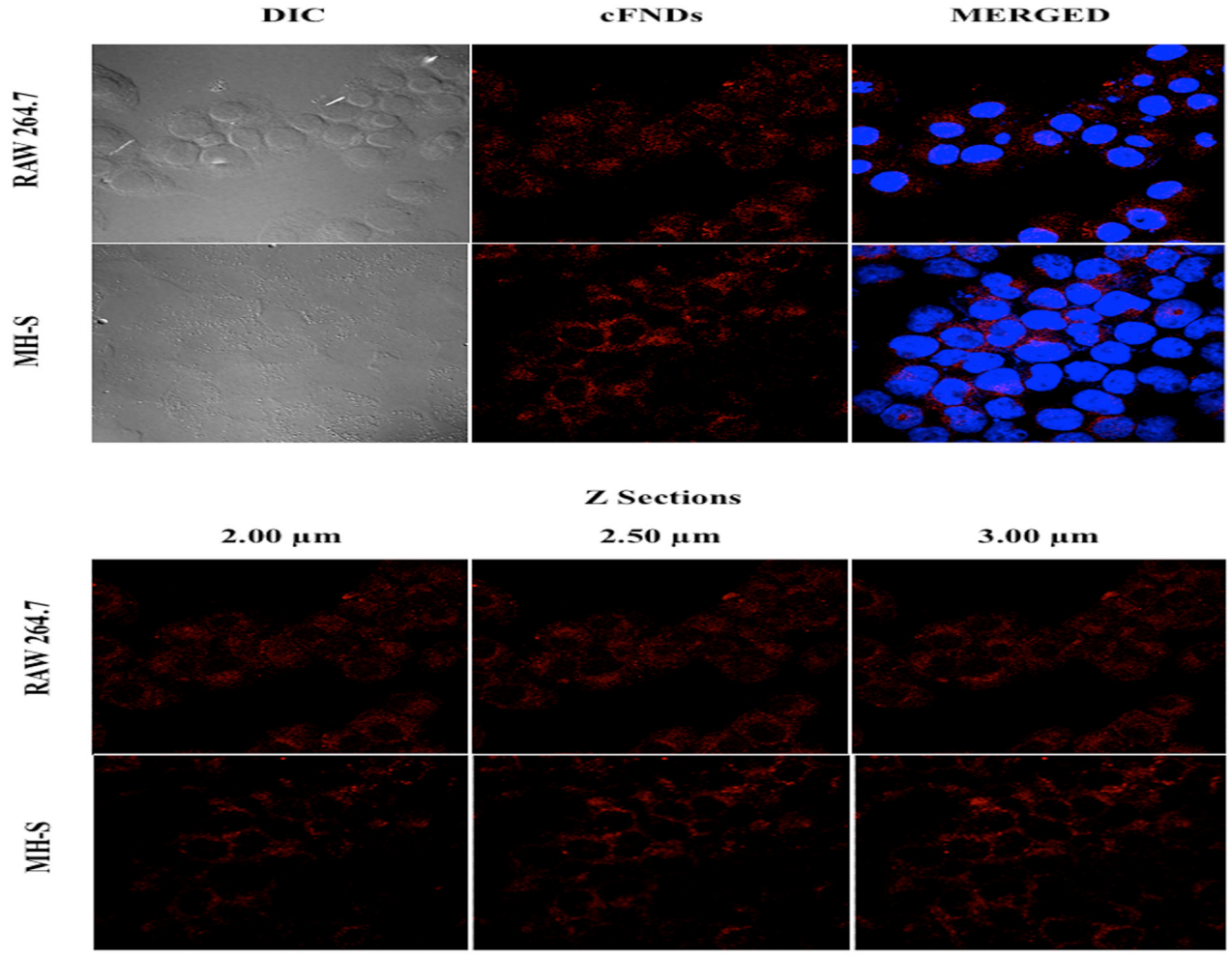

Figure 1: Uptake and localization of cFNDs by macrophages.

RAW 264.7/MH-S cells [0.1×106/ml/well] were cultured with cFNDs (10 µg/ml) for 12 hours. After incubation, cells were washed with PBS and examined by confocal microscopy. Internalization of cFNDs by RAW 264.7 and MH-S cells for 12-hour time point are shown in the top panels. Red fluorescence denotes cFNDs uptake and blue stain of Hoechst 33342 dye shows the nuclei. Magnification 100X in all cases. Z-sectioning results at various depths showing the internalization of cFNDs are shown in the bottom panel.

Inhibition of BCG induced Reactive Oxygen Species (ROS) production by cNDs

Onset of inflammatory response in macrophages is characterised by huge upsurge in production of ROS inside the cells (33). ROS production by the macrophage cell lines in response to BCG and its modulation by cNDs was studied by using the fluorogenic dye 2',7'-Dichlorofluorescin diacetate (DCFDA) that gets converted to a fluorescent product DCF in presence of ROS, as described elsewhere (34). Results presented in Figure 2 clearly show that little or no ROS production was observed in untreated control macrophages or macrophages treated with cNDs alone. Treatment with autoclaved BCG resulted in marked increase in ROS production by macrophages ($p<0.001$) with almost 100 percent positivity and a 10 to 14 fold increase in DCF MFI (mean fluorescence intensity) that would be a measure of relative average per cell production of ROS. BCG induced ROS response was almost completely blocked in presence of cNDs (85% and 90% inhibition in RAW 264.7 and MH-S cells respectively in case of DCF percent positive cells and 90% and 85% inhibition in RAW 264.7 and MH-S cells respectively in DCF MFI). These results show that cNDs can block the BCG induced ROS production in macrophages.

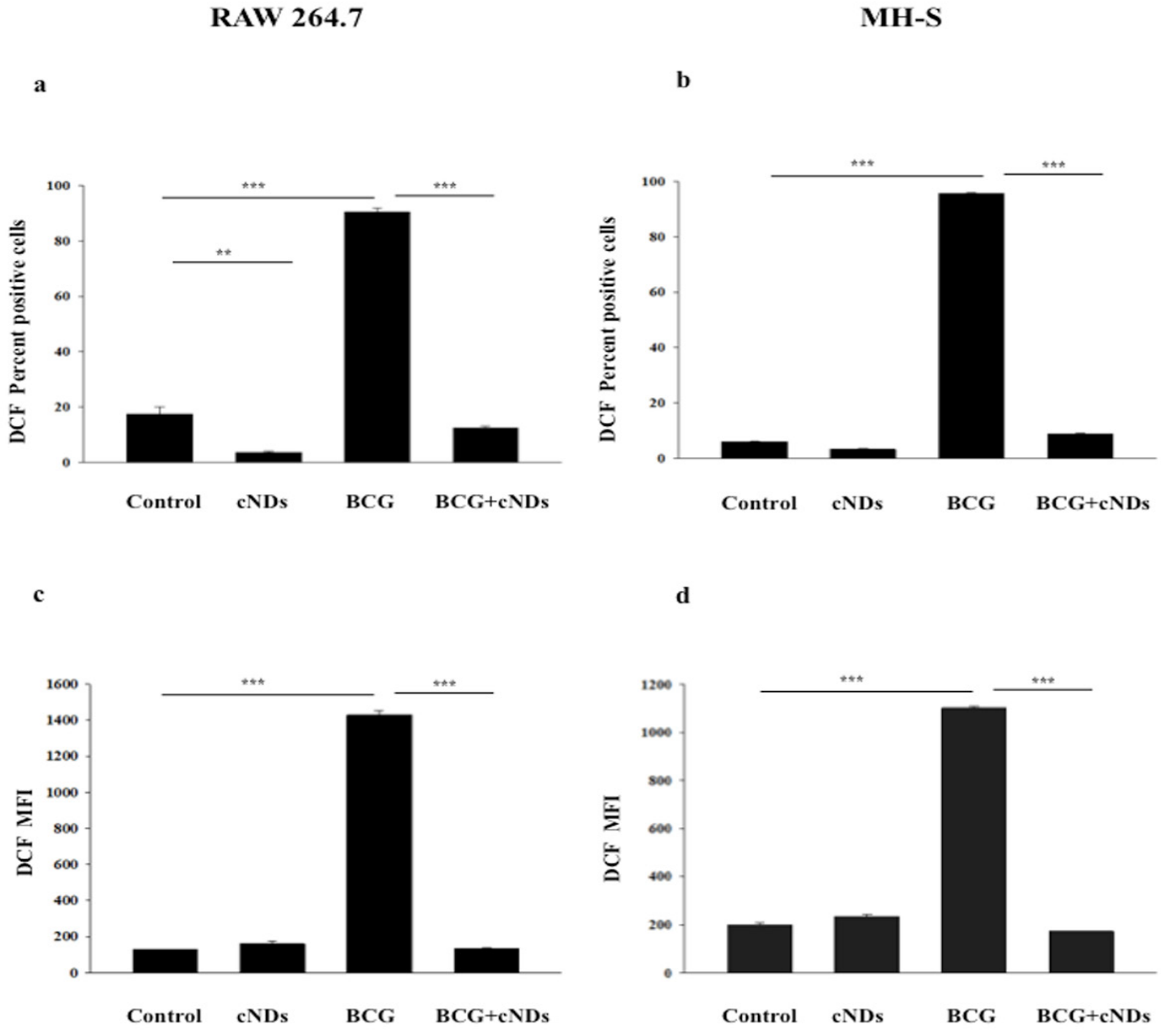

Figure 2: Inhibition of BCG induced ROS production by cNDs.

RAW 264.7 and MH-S cells [0.1×106/ml/well] were cultured alone or with cNDs (100 µg/ml), BCG (MOI 100:1) and BCG + cNDs for 12 hours. After incubation, cells were harvested, stained with 5 µM DCFDA for 30 minutes, washed and analyzed by flow cytometry. Panel a and b represent DCF Percent positive cells while panel c and d represent DCF MFI for RAW 264.7 and MH-S respectively. Histograms show result of 3 independent experiments (Mean ±SEM). **p<0.01, ***p<0.001.

Reduction of BCG induced nitric oxide production by cNDs

Nitric oxide has been demonstrated to be a crucial molecule in mediating inflammatory responses in macrophages and other cells of the immune system (35). Results in Figure 3a (RAW 264.7 cells) and 3b (MH-S cells) show that in control macrophages or macrophages treated with cNDs alone for 4 and 12h time points, there was little secretion of NO. Treatment with autoclaved BCG led to a substantial increase in NO production in both the macrophage cell lines ($p<0.001$) which was strongly inhibited in presence of cNDs; the decline being 90% and 75% in 4 hour and 12 hour time point in RAW 264.7 cells and 75% and 80% in both 4 hour and 12 hour time points in MH-S cells respectively.

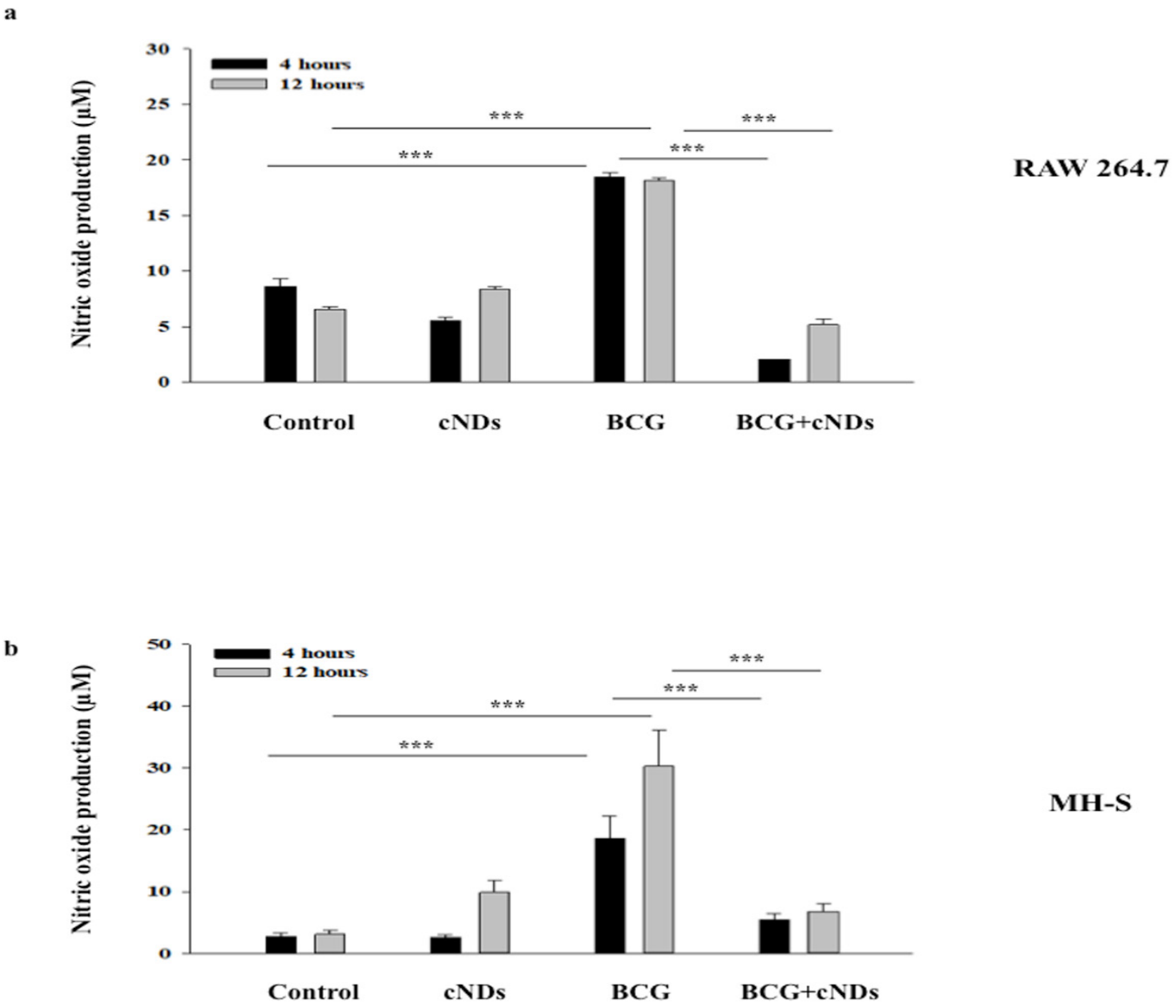

Figure 3: Suppression of BCG induced NO production by cNDs.

RAW 264.7 and MH-S cells [0.1×106/ml/well] were cultured alone or with cNDs (100µg/ml), BCG (MOI 100:1) and BCG + cNDs for 4 hours and 12 hours. NO levels in the culture supernatants were measured by using modified Griess reagent as described in Methods. Histograms show result of 3 independent experiments (Mean±SEM).***$p<0.001$.

Regulation of expression of BCG induced pro-inflammatory genes in macrophages by cNDs

Since we found a strong suppressive effect of cNDs in downregulating BCG induced ROS and NO, we further tested the effect of BCG on early expression of some crucial key genes known to be involved in the generation of inflammatory response, namely COX-2, iNOS, TNF-α, IL-6 and IL-1β and modulation of their expression in presence of cNDs. Results in Figure 4 show that treatment of RAW 264.7 and MH-S cells with BCG for 4h resulted in a significant increase in expression of COX-2, iNOS, TNF-α, IL-6 and IL-1β. While in most cases the increase ranged from 2 to 15 fold, the enhancement of expression of IL-6 and IL-1β in RAW 264.7 cells was 200 and 70 fold respectively.

However, treatment of both RAW 264.7 and MH-S cells with cNDs led to a remarkable reduction in expression level of all BCG induced pro-inflammatory genes; the decline being 50% in COX-2($p<0.01$) and iNOS($p<0.05$) and 80% in TNF-α ($p<0.001$), IL-6 ($p<0.001$)and IL-1β ($p<0.01$) in RAW 264.7 cells. The corresponding decline in MH-S was nearly 80% in COX-2 ($p<0.001$), iNOS($p<0.001$), TNF-α ($p<0.01$), IL-6 ($p<0.05$) and IL-1β($p<0.05$).

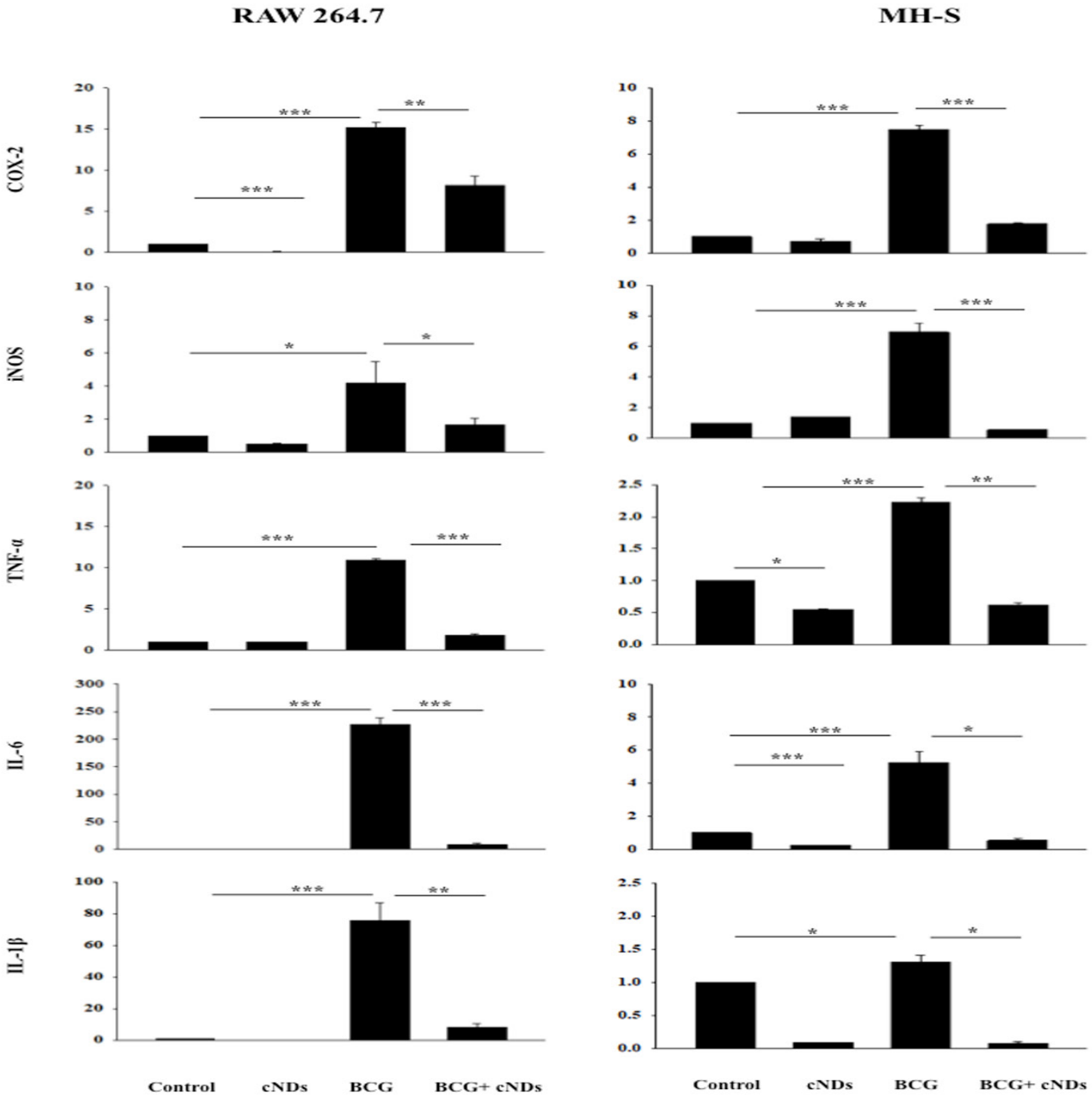

Figure 4: Modulation of expression of BCG induced pro-inflammatory genes by cNDs.

RAW 264.7/MH-S cells [0.5×106/ml/well] were cultured alone or with cNDs (100 µg/ml), BCG (MOI 100:1) and BCG + cNDs for 4 hours. RNA was extracted and RTPCR was performed as described in Methods. Fold change in gene expression was calculated using 2–ΔΔCt method. Histograms show result of 3 independent experiments (Mean± SEM). *p<0.05, **p<0.01, ***p<0.001.

Inhibition of expression of BCG induced COX-2 enzyme at protein level by cNDs

Cyclooxygenase-2 (COX-2) is a key enzyme involved in the conversion of arachidonic acid to several molecules of prostaglandin family that in turn play a crucial role in the induction of inflammatory responses (36). Our RT-PCR results showed downregulation of BCG induced expression of COX-2 gene at transcriptional level in the presence of cNDs. Effect of cNDs on the accumulation of COX-2 enzyme at the translational level in the macrophage cells was also assessed using Western blotting technique. COX-2 is an inducible enzyme and accordingly there was no expression of COX-2 in untreated control RAW 267.4 and MH-S cells (Figure 5). Treatment with cNDs alone also did not induce COX-2 in these cells but BCG induced a marked accumulation of COX-2 enzyme in both cell lines that was strongly inhibited by cNDs treatment (60% and 99% inhibition in RAW 264.7 and MH-S cells respectively).

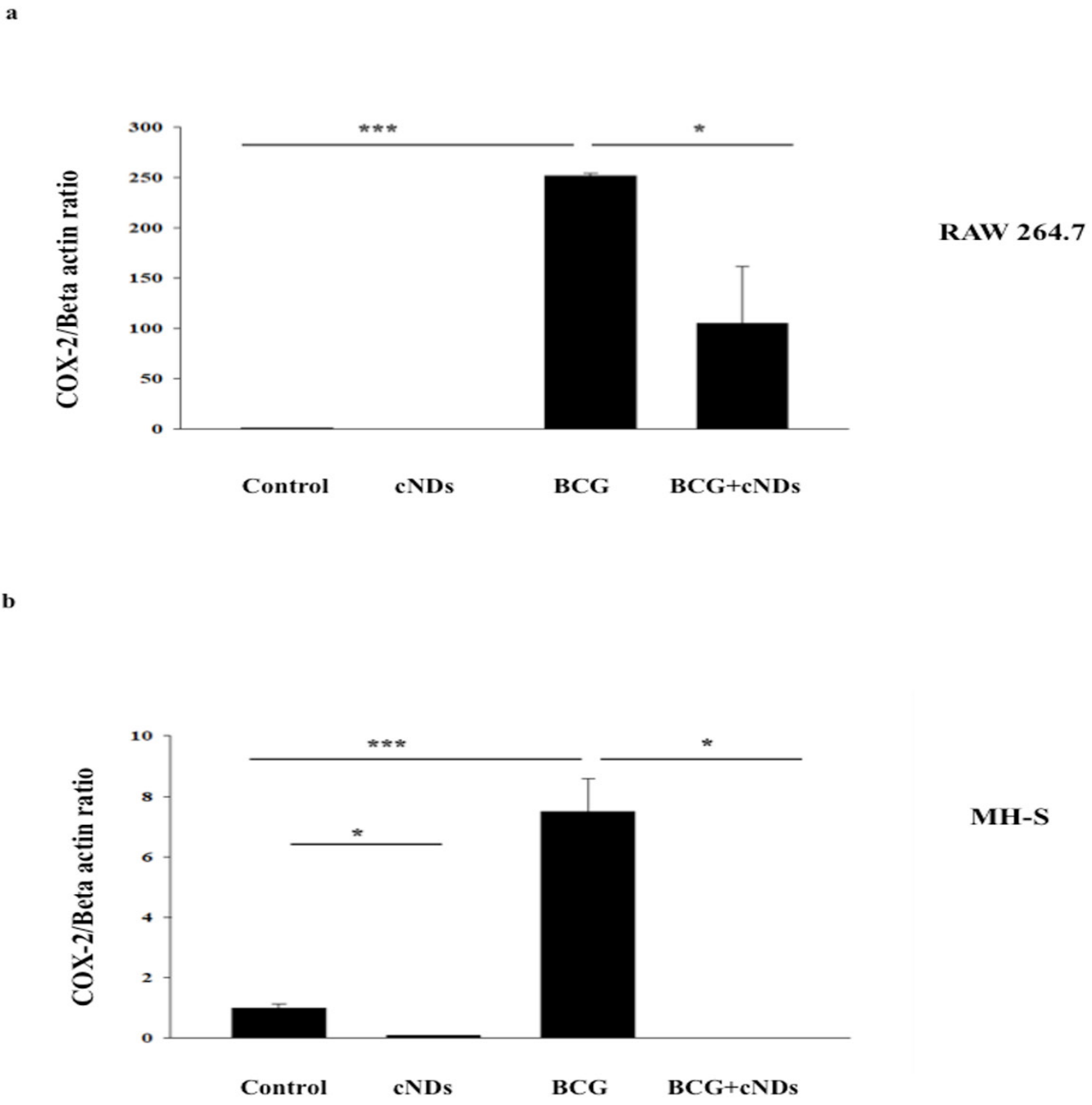

Figure 5: Modulation of expression of BCG induced COX-2 by cNDs using Western blotting. RAW 264.7 and MH-S cells [0.5 × 106/ml/well] were cultured alone or with 100 µg/ml cNDs, BCG MOI 100:1 and BCG MOI 100:1+100 µg/ml cNDs for 24 hours. Protein lysates were prepared by using RIPA extraction buffer and Western blotting carried out to estimate COX-2 gene product as described in Methods. Panel a and Panel b show histograms for COX-2 normalized with housekeeping gene Beta actin for RAW 264.7 and MH-S cells respectively. Histograms show result of 3 independent experiments (Mean± SEM). *p<0.05, ***p<0.001.

Modulation of expression of BCG induced MMP-2 and MMP-9 by cNDs

Matrix metallopeptidases (MMPs) have been demonstrated to be important mediators in regulation of inflammation responses (37). Secretion of two of the crucial members of the MMPs family of metallopeptidases, MMP-2 and MMP-9 was assessed for macrophage cell lines treated with BCG in presence and absence of cNDs. Using the technique of Gelatin Zymography we found a basal release of MMP-2 and MMP-9 in the culture supernatants of control RAW 267.4 and MH-S cells, that was significantly increased upon treatment of the cells with BCG (Figure 6). This enhanced MMP-2 and MMP-9 secretion was reversed if cNDs were added along with BCG wherein the MMP secretions were brought down to a level similar to control cultures (Figure 6).

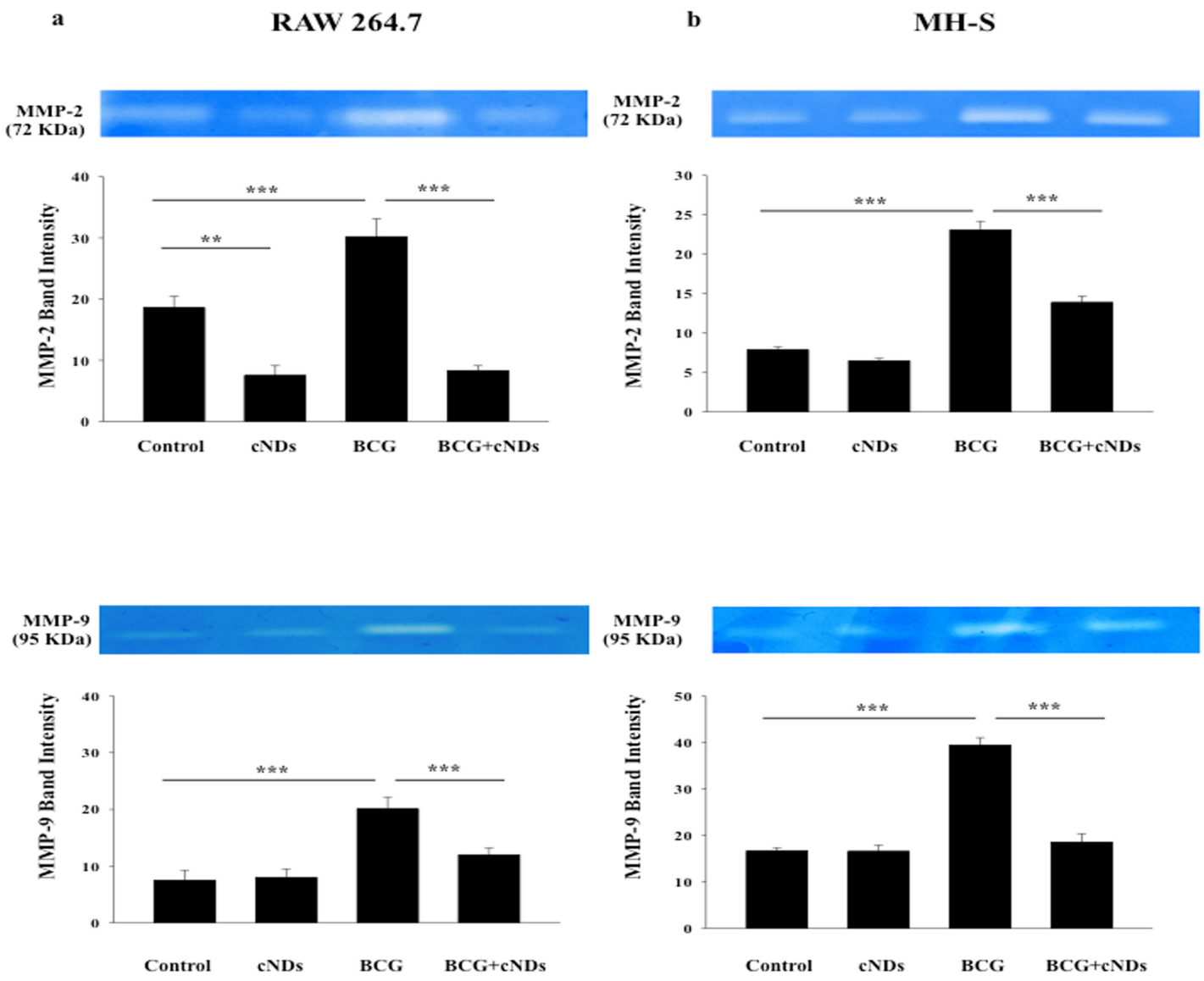

Figure 6: Modulation of BCG induced MMP-2 and MMP-9 by cNDs.

RAW 264.7 and MH-S cells [0.5 × 106/ml/well] were cultured alone or with cNDs (100 µg/ml), BCG (MOI 100:1) and BCG + cNDs for 12 hours in serum free medium. Culture supernatants were used for Gelatin zymography to reveal different MMPs as described in Methods. Panel a and b show results for RAW 264.7 cells and MH-S cells respectively. Histograms show result of 3 independent experiments (Mean ± SEM). **p<0.01, ***p<0.001.

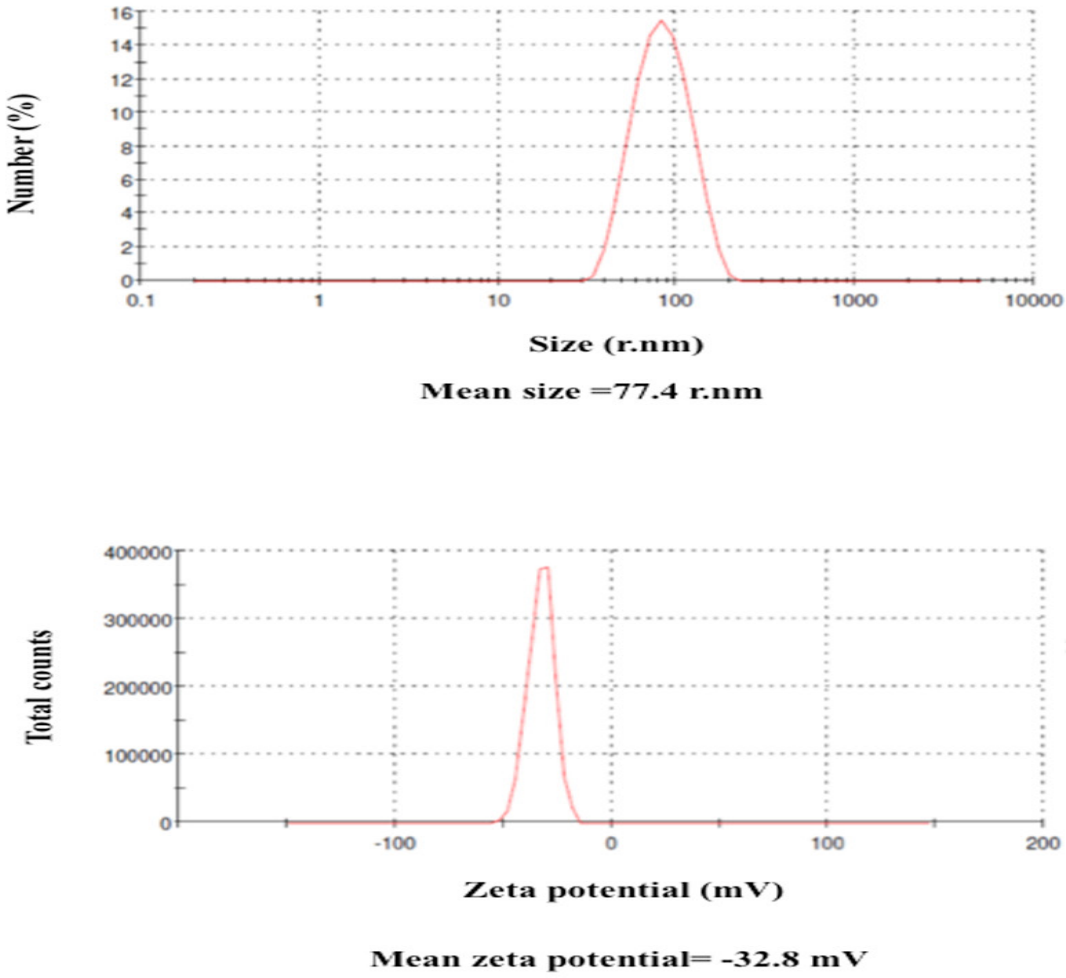

Supplementary Figure 1: Characterization of cFNDs using Zetasizer.
Upper panel shows the Zeta size and lower panel shows the Zeta potential of cFNDs measured using Malvern Zetasizer.

Discussion

Inflammatory process is induced in response to the external challenge of pathogens and is an effective mechanism to clear the system of the pathogens. Many of the effector molecules that are secreted by inflammatory cells are nonspecific in nature may cause considerable tissue damage. A resolution phase of inflammatory response follows in which tissue repair takes place. Macrophages play a central role in the inductive as well as resolution phases of inflammation. Macrophages exist in appropriately polarized states depending upon the function they perform. M1 macrophages are involved in the induction of inflammation and M2 category of macrophages are required during the later resolution phase of the inflammatory response (38). An unresolved and sustained inflammatory response (chronic inflammation) may cause serious damage to tissues that may be lethal. Understanding the factors that regulate inflammatory response is therefore important and there is a need to find drugs and agents that suppress the inflammatory response when it threatens serious damage to tissues and cells at the site of inflammation. A potential candidate for suppressing inflammation is nanodiamonds (NDs) and the basic focus of this paper is to assess the efficacy of NDs to regulate inflammatory processes at the level of macrophages. M1 polarized macrophages should be used for such study as this stage participates in the induction of inflammation. Both RAW 264.7 and MH-S macrophage cell lines that we used in this study essentially represent the M1 polarized stage (39-43), as is confirmed in our study showing that the test pathogen BCG induced a large number of pro-inflammatory molecules that participate in the induction and effector phases of inflammatory response. The parameters that we used to assess the inflammatory response in the two immortalized mouse macrophage cell lines (44) included enzymes cyclooxygenase-2 (COX-2)

and inducible nitric oxide synthetase (iNOS) that are crucial to generate reactive oxygen species (ROS) and nitric oxide (NO) that are involved in the effector phase of the inflammatory response (45-49). Gene expression of both these enzymes assessed by RTPCR was markedly upregulated in BCG treated cells and was in turn strongly inhibited by treatment with cNDs. Western blotting techniques confirmed the increased cellular concentration of the enzyme cyclooxygenase in response to BCG and its down regulation in presence of cNDs. COX-2 and iNOS enzymes are required for the generation of ROS and nitric oxide involved in the effector phase of the inflammatory process (45-49) and accordingly, secretion of ROS and nitric oxide by the two cell lines in presence of cNDs indicated that the cNDs may have strong anti-inflammatory properties. Besides these parameters, we also assessed the gene expression of the cytokines TNF-α, IL-6 and IL-1β that are key mediators of inflammation (50-52). All these cytokines too were strongly induced by BCG and blocked by the addition of cNDs.

Secretion of matrix metallopeptidases (MMPs) i.e. MMP-2 and MMP-9 is an important feature of inflammatory responses since these enzymes can convert inactive pro-cytokine proteins to active pro-inflammatory cytokines (53, 54) and play an important role in tissue remodelling following an inflammatory response (55). Using the Gelatin zymography technique, the secretion of these two enzymes by the macrophage cell lines too was found to be augmented by BCG and the increase blocked by cNDs. In previous studies by our group, acid-functionalized single-walled carbon nanotubes (AF-SWCNTs), another form of carbon nanoparticles, were shown to have suppressive effect on a variety of immune functions like B cell activation, T cell and NK cell activation, antigen presentation (26, 56-60, 63) and hematopoiesis (61, 62). Interestingly, activated immune cells internalized more AF-SWCNTs than the control resting cells (63). Functionalized nanodiamonds (carboxy nanodiamonds functionalized by octadecylamine and dexamethasone) were shown to have an inhibitory effect on the inflammatory response in human peripheral blood monocytes (64). Our present study shows that carboxylated NDs without coupling to any drug could downregulate inflammatory responses in mouse macrophage cell lines. Carbon nanoparticles may therefore constitute a potential class of immunosuppressive agents perhaps because of their better uptake by activated immune cells including macrophages (63, 65). NDs are in general non-toxic to cells in vitro and in vivo (12, 16-23) and do not constitute a known health risk. Further, NDs may naturally target macrophages since these cells have an inherent phagocytic activity to internalize particulate matter. In view of our results showing strong anti-inflammatory effect, nanodiamonds may be examined as a potential anti-inflammatory agent. This proposition would require further exploration.

Funding

This work was supported by Department of Science and Technology, Government of India, Nano-sciences Mission grant number SR/NM/NS-1219 and JC Bose award to RKS. DB received fellowship support from the Department of Biotechnology, New Delhi.

Conflict of Interest

Authors declare that they have no conflict of interest.

Acknowledgements

Research funding from the Department of Science and Technology, Government of India, and fellowship support to DB from DBT are gratefully acknowledged.

References

1. Chao JI, Perevedentseva E, Chung PH, Liu KK, Cheng CY, Chang CC, Cheng CL. Nanometer-sized diamond particle as a probe for biolabeling. Biophys J.2007 Sep 15; 93(6): 2199-208.

2. Dolmatov VY. Detonation-synthesis nanodiamonds: synthesis, structure,properties and applications. Russ Chem Rev. 2007; 76(4): 339-360.

3. Mochalin VN, Shenderova O, Ho D, Gogotsi Y. The properties and applications of nanodiamonds. Nat Nanotechnol. 2012 Jan; 7(1): 11-23.

4. Pichot V, Muller O, Seve A, Yvon A, Merlat L, Spitzer D. Optical properties of functionalized nanodiamonds. Sci Rep. 2017 Oct 26; 7(1): 1-8.

5. Prabhakar N, Rosenholm JM. Nanodiamonds for advanced optical bioimaging and beyond. Curr Opin Colloid Interface Sci. 2019 Feb 1; 39: 220-31.

6. Hemelaar SR, De Boer P, Chipaux M, Zuidema W, Hamoh T, Martinez FP, Nagl A, Hoogenboom JP, Giepmans BN, Schirhagl R. Nanodiamonds as multi-purpose labels for microscopy. Sci Rep. 2017 Apr 7; 7(1): 1-9.

7. Passeri D, Rinaldi F, Ingallina C, Carafa M, Rossi M, Terranova ML, Marianecci C. Biomedical applications of nanodiamonds: an overview. J Nanosci.Nanotechnol. 2015 Feb 1; 15(2): 972-88.

8. Turcheniuk K, Mochalin VN. Biomedical applications of nanodiamond. Nanotechnology. 2017 Jun 1; 28(25): 252001.

9. Chang YR, Lee HY, Chen K, Chang CC, Tsai DS, Fu CC, Lim TS, Tzeng YK,Fang CY, Han CC, Chang HC. Mass production and dynamic imaging of fluorescent nanodiamonds. Nat Nanotechnol.2008 May; 3(5):284-8.

10. Fu CC, Lee HY, Chen K, Lim TS, Wu HY, Lin PK, Wei PK, Tsao PH, Chang HC, Fann W. Characterization and application of single fluorescent nanodiamonds as cellular biomarkers. Proc Natl Acad Sci U S A. 2007 Jan 16;104(3): 727-32.

11. Vaijayanthimala V, Cheng PY, Yeh SH, Liu KK, Hsiao CH, Chao JI, Chang HC.The long-term stability and biocompatibility of fluorescent nanodiamond as an in vivo contrast agent. Biomaterials. 2012 Nov 1; 33(31): 7794-802.

12. Mohan N, Chen CS, Hsieh HH, Wu YC, Chang HC. In vivo imaging andtoxicity assessments of fluorescent nanodiamonds in Caenorhabditis elegans. Nano Lett. 2010 Sep 8; 10(9): 3692-99.

13. Liu W, Naydenov B, Chakrabortty S, Wuensch B, Hübner K, Ritz S, Cölfen H, Barth H, Koynov K, Qi H, Leiter R. Fluorescent nanodiamond–gold hybrid particles for multimodal optical and electron microscopy cellular imaging. Nano Lett. 2016 Oct 12; 16(10): 6236-44.

14. Rehor I, Lee KL, Chen K, Hajek M, Havlik J, Lokajova J, Masat M, Slegerova J, Shukla S, Heidari H, Bals S. Plasmonic nanodiamonds: Targeted core–shell type nanoparticles for cancer cell thermoablation. Adv Healthc Mater. 2015 Feb; 4(3): 460-8.

15. Ginés L, Mandal S, Cheng CL, Sow M, Williams OA. Positive zeta potential of nanodiamonds. Nanoscale. 2017; 9(34): 12549-55.

16. Tsai LW, Lin YC, Perevedentseva E, Lugovtsov A, Priezzhev A, Cheng CL. Nanodiamonds for medical applications: interaction with blood in vitro and in vivo. Int J Mol Sci. 2016 Jul; 17(7): 1111.

17. Chow EK, Zhang XQ, Chen M, Lam R, Robinson E, Huang H, Schaffer D, Osawa E, Goga A, Ho D. Nanodiamond therapeutic delivery agents mediate enhanced chemoresistant tumor treatment. Sci Transl Med. 2011 Mar 9; 3(73): 73ra21.

18. Yuan Y, Wang X, Jia G, Liu JH, Wang T, Gu Y, Yang ST, Zhen S, Wang H, Liu Y. Pulmonary toxicity and translocation of nanodiamonds in mice. Diam Relat Mater. 2010 Apr 1; 19(4): 291-9.

19. Yu SJ, Kang MW, Chang HC, Chen KM, Yu YC. Bright fluorescent nanodiamonds: no photobleaching and low cytotoxicity. J Am Chem Soc. 2005 Dec 21; 127(50): 17604-5.

20. Schrand AM, Dai L, Schlager JJ, Hussain SM, Osawa E. Differential biocompatibility of carbon nanotubes and nanodiamonds. Diam Relat Mater. 2007 Dec 1; 16(12): 2118-23.

21. Moore L, Grobárová V, Shen H, Man HB, Míčová J, Ledvina M, Štursa J, Nesladek M, Fišerová A, Ho D. Comprehensive interrogation

of the cellular response to fluorescent, detonation and functionalized nanodiamonds. Nanoscale.2014; 6(20): 11712-21.
22. Hsu TC, Liu KK, Chang HC, Hwang E, Chao JI. Labeling of neuronal differentiation and neuron cells with biocompatible fluorescent nanodiamonds. Sci Rep. 2014 May 16; 4:5004.
23. Liu KK, Cheng CL, Chang CC, Chao JI. Biocompatible and detectable carboxylated nanodiamond on human cell. Nanotechnology. 2007 Jul 13; 18(32): 325102.
24. Zhou Y, Hong Y, Huang H. Triptolide attenuates inflammatory response in membranous glomerulo-nephritis rat via downregulation of NF-κB signaling pathway. Kidney Blood Press R. 2016; 41(6): 901-10.
25. Fujiwara N, Kobayashi K. Macrophages in inflammation. Curr Drug Targets Inflamm Allergy. 2005; 4(3): 281-286.
26. Dutt TS, Mia MB, Saxena RK. Elevated internalization and cytotoxicity of polydispersed single-walled carbon nanotubes in activated B cells can be basis for preferential depletion of activated B cells in vivo. Nanotoxicology. 2019 Jul 3; 13(6): 849-60.
27. Saxena RK, Saxena QB, Weissman DN, Simpson JP, Bledsoe TA, Lewis DM. Effect of diesel exhaust particulate on Bacillus Calmette-Guerin lung infection in mice and attendant changes in lung interstitial lymphoid subpopulations and IFNγ response. Toxicol Sci. 2003 May 1; 73(1): 66-71.
28. Nolan T, Hands RE, Bustin SA. Quantification of mRNA using real-time RTPCR. Nat Protoc. 2006 Aug; 1(3): 1559-82.
29. Singh AP, Mia MB, Saxena RK. Acid-functionalized single-walled carbon nanotubes alter epithelial tight junctions and enhance paracellular permeability. J
Biosci. 2020 Dec 1; 45(1): 23.
30. Toth M, Fridman R. Assessment of Gelatinases (MMP-2 and MMP-9) by Gelatin Zymography. Methods Mol Med. 2001; 57: 163-174.
31. Kumari M, Saxena RK. Relative efficacy of uptake and presentation of Mycobacterium bovis BCG antigens by type I mouse lung epithelial cells and peritoneal macrophages. Infect Immun. 2011 Aug 1; 79(8): 3159-67.
32. Ghosh S, Saxena RK. Early effect of Mycobacterium tuberculosis infection on Mac-1 and ICAM-1 expression on mouse peritoneal macrophages. Exp Mol Med. 2004 Oct; 36(5): 387-95.
33. Forrester SJ, Kikuchi DS, Hernandes MS, Xu Q, Griendling KK. Reactive oxygen species in metabolic and inflammatory signaling. Circ Res. 2018 Mar 16; 122(6): 877-902.
34. Eruslanov E, Kusmartsev S. Identification of ROS using oxidized DCFDA and flow-cytometry. Methods Mol Biol. 2010; 594: 57-72.
35. Laroux FS, Pavlick KP, Hines IN, Kawachi S, Harada H, Bharwani S, Hoffman JM, Grisham MB. Role of nitric oxide in inflammation. Acta Physiol. Scand. 2001 Sep; 173(1): 113-8.
36. Williams CS, Mann M, DuBois RN. The role of cyclooxygenases in inflammation, cancer, and development. Oncogene. 1999 Dec; 18(55): 7908-16.
37. Müller-Quernheim J. MMPs are regulatory enzymes in pathways of inflammatory disorders, tissue injury, malignancies and remodelling of the lung. Eur Respir J. 2011; 38(1): 12-14
38. Mosser DM, Edwards JP. Exploring the full spectrum of macrophage activation. Nat Rev Immunol. 2010 Dec; 8(12): 958-69.
39. Bansal K, Narayana Y, Patil SA, Balaji KN. M. bovis BCG induced expression of COX-2 involves nitric oxide-dependent and-independent signaling pathways. J Leukoc Biol. 2009 May; 85(5): 804-16.
40. Chávez-Galán L, Vesin D, Martinvalet D, Garcia I. Low dose BCG infection as a model for macrophage activation maintaining cell viability. J Immunol Res. 2016 Oct 19; 4048235.
41. Kan LL-Y, Liu D, Chan BC-L, et al. The flavonoids of Sophora flavescens exerts anti-inflammatory activity via promoting autophagy of Bacillus Calmette-Guérinstimulated macrophages. J Leukoc Biol. 2020; 1– 16.
42. Tweedie D, Luo W, Short RG, Brossi A, Holloway HW, Li Y, Yu QS, Greig NH. A cellular model of inflammation for identifying TNF-α synthesis inhibitors. J Neurosci Methods. 2009 Oct 15; 183(2): 182-187.
43. Knapp S, Florquin S, Golenbock DT, van der Poll T. Pulmonary lipopolysaccharide (LPS)-binding protein inhibits the LPS-induced lung inflammation in vivo. J Immunol. 2006 Mar 1; 176(5): 3189-95.
44. Chamberlain LM, Godek ML, Gonzalez-Juarrero M, Grainger DW. Phenotypic non-equivalence of murine (monocyte-) macrophage cells in biomaterial and inflammatory models. J Biomed Mater Res A. 2009; 88(4): 858-871.
45. Suschek CV, Schnorr O, Kolb-Bachofen V. The role of iNOS in chronic inflammatory processes in vivo: is it damage-promoting, protective, or active at all?. Curr Mol Med. 2004 Nov 1; 4(7): 763-75.
46. Mittal M, Siddiqui MR, Tran K, Reddy SP, Malik AB. Reactive oxygen species in inflammation and tissue injury. Antioxid Redox Signal. 2014 Mar 1; 20(7): 1126-67.
47. Ricciotti E, FitzGerald GA. Prostaglandins and inflammation. Arterioscler Thromb Vasc Biol. 2011 May; 31(5): 986-1000.
48. Seibert K, Masferrer JL. Role of inducible cyclooxygenase (COX-2) in inflammation. Receptor. 1994; 4(1): 17-23.
49. Murakami A, Ohigashi H. Targeting NOX, INOS and COX-2 in inflammatory cells: chemoprevention using food phytochemicals. Int J Cancer. 2007 Dec 1; 121(11): 2357-63.
50. Zelová H, Hošek J. TNF-α signalling and inflammation: interactions between old acquaintances. Inflamm Res. 2013 Jul 1; 62(7): 641-51.
51. Choy E, Rose-John S. Interleukin-6 as a multifunctional regulator: inflammation, immune response, and fibrosis. J Scleroderma Relat Disord. 2017; 2(2_suppl): S1-S5.
52. Dinarello CA. Overview of the IL-1 family in innate inflammation and acquired immunity. Immunol Rev. 2018 Jan; 281(1): 8-27.
53. Black RA, Rauch CT, Kozlosky CJ, Peschon JJ, Slack JL, Wolfson MF, Castner BJ, Stocking KL, Reddy P, Srinivasan S, Nelson N. A metalloproteinase disintegrin that releases tumour-necrosis factor-α from cells. Nature. 1997 Feb; 385(6618): 729-733.
54. Ito A, Mukaiyama A, Itoh Y, Nagase H, Thøgersen IB, Enghild JJ, Sasaguri Y, Mori Y. Degradation of interleukin 1β by matrix metalloproteinases. J Biol Chem. 1996 Jun 21; 271(25): 14657-60.
55. Page-McCaw A, Ewald AJ, Werb Z. Matrix metalloproteinases and the regulation of tissue remodelling. Nat Rev Mol Cell Biol. 2007 Mar; 8(3): 221-33.
56. Alam A, Sachar S, Puri N, Saxena RK. Interactions of polydispersed singlewalled carbon nanotubes with T cells resulting in downregulation of allogeneic CTL responses in vitro and in vivo. Nanotoxicology. 2013 Dec 1; 7(8): 1351-60.
57. Mia MB, Saxena RK. Poly dispersed acid-functionalized single walled carbon nanotubes target activated T and B cells to suppress acute and chronic GVHD in mouse model. Immunol Lett. 2020 Jun 3; 30-37.
58. Alam A, Puri N, Saxena RK. Uptake of poly-dispersed single-walled carbon nanotubes and decline of functions in mouse NK cells undergoing activation. J Immunotoxicol. 2016 Sep 2; 13(5): 758-65.
59. Kumari M, Sachar S, Saxena RK. Loss of proliferation and antigen presentation activity following internalization of polydispersed carbon nanotubes by primary lung epithelial cells. PloS one. 2012 Feb 27; 7(2): e31890.
60. Rizvi ZA, Puri N, Saxena RK. Lipid antigen presentation through CD1d pathway in mouse lung epithelial cells, macrophages and dendritic cells and its suppression by poly-dispersed single-walled carbon nanotubes. Toxicol In Vitro. 2015 Sep 1; 29(6): 1275-82.

61. Sachar S, Saxena RK. Cytotoxic effect of poly-dispersed single walled carbon nanotubes on erythrocytes in vitro and in vivo. PLoS One. 2011 Jul 19; 6(7): e22032.
62. Bhardwaj N, Saxena RK. Selective loss of younger erythrocytes from blood circulation and changes in erythropoietic patterns in bone marrow and spleen in mouse anemia induced by poly-dispersed single-walled carbon nanotubes. Nanotoxicology. 2015 Nov 17; 9(8): 1032-40.
63. Dutt TS, Saxena RK. Activation of T and B lymphocytes induces increased uptake of poly-dispersed single-walled carbon nanotubes and enhanced cytotoxicity. Int J Nano Med & Eng. 2019 Jul; 4(3): 16-25.
64. Pentecost AE, Witherel CE, Gogotsi Y, Spiller KL. Anti-inflammatory effects of octadecylamine-functionalized nanodiamond on primary human macrophages. Biomater Sci. 2017; 5(10): 2131-43.
65. Dutt TS, Saxena RK. Uptake of Carboxylated Fluorescent Nano-Diamonds by Resting and Activated T and B Lymphocytes and Comparison with Carbon Nanotube Uptake. Int J Nano Med & Eng. 2019 Dec; 4(7).